LAWRENCE
LIVERMORE
NATIONAL
LABORATORY

LLNL-CONF-456824

Driving Toroidally Asymmetric Current Through the Tokamak Scrape-Off Layer to Control Edge-Localized Instabilities and Equilibrium Profiles

I. Joseph, R. H. Cohen, T. W. Petrie, T. D. Rognlien, D. D. Ryutov, G. M. Staebler, H. Takahashi, S. J. Zweben

September 24, 2010

2010 International Atomic Energy Agency Fusion Energy Conference
Daejeon, South Korea
October 11, 2010 through October 16, 2010

Disclaimer

This document was prepared as an account of work sponsored by an agency of the United States government. Neither the United States government nor Lawrence Livermore National Security, LLC, nor any of their employees makes any warranty, expressed or implied, or assumes any legal liability or responsibility for the accuracy, completeness, or usefulness of any information, apparatus, product, or process disclosed, or represents that its use would not infringe privately owned rights. Reference herein to any specific commercial product, process, or service by trade name, trademark, manufacturer, or otherwise does not necessarily constitute or imply its endorsement, recommendation, or favoring by the United States government or Lawrence Livermore National Security, LLC. The views and opinions of authors expressed herein do not necessarily state or reflect those of the United States government or Lawrence Livermore National Security, LLC, and shall not be used for advertising or product endorsement purposes.

Driving Toroidally Asymmetric Current Through the Tokamak Scrape-Off Layer to Control Edge-Localized Instabilities and Equilibrium Profiles

I. Joseph 1), R. H. Cohen 1), T.W. Petrie 2), T. D. Rognlien 1), D. D. Ryutov 1),
G. M. Staebler 2), H. Takahashi 3), S. J. Zweben 3)

1) Lawrence Livermore National Laboratory, Livermore, California, USA
2) General Atomics, San Diego, California, USA
3) Princeton Plasma Physics Laboratory, Princeton, New Jersey, USA

email: joseph5@llnl.gov

Abstract. A critical requirement for tokamak fusion reactors is the control of the divertor heat load, both the time-averaged value and the impulsive fluxes that accompany edge-localized modes (ELMs). The prediction for ITER is that ELMs will impulsively deliver extremely high heat fluxes to bounding wall components. For larger devices, even the steady-state fluxes can become unacceptably large. We propose driving toroidally non-axisymmetric current through the scrape-off layer (SOL) plasma both to broaden the SOL by driving radial convection and to control the edge pressure gradient by driving resonant magnetic perturbations (RMPs). Electrostatic convection generated by electric biasing has been shown to locally spread the SOL plasma on both MAST and NSTX, and on MAST, this technique was shown to reduce the peak heat flux at the target plate. First results of experiments to test the effect on the NSTX divertor are reported below. Experimentally, RMPs from external coils have been demonstrated to produce sufficient transport to control ELM stability. Choosing the appropriate width and phasing of the biasing region at the target plate optimize the RMP amplitude generated by the SOL current. Longer wavelength modes produce a larger effect because they are not sheared as strongly by the X-point. Generation of the necessary currents is challenging due to the possibly substantial power requirements and the possible need for internal insulators. We analyze passive current-drive mechanisms that rely on puffing and pumping of neutral gas and/or impurities in a toroidally asymmetric fashion using the UEDGE code to model the ITER divertor.

1. Introduction

A critical requirement for high-performance tokamak reactors is the control of the divertor heat load, both the time-averaged flux and the impulsive bursts that accompany edge plasma instabilities. The prediction for ITER is that extremely high heat fluxes will be impulsively delivered to divertor target plates and bounding wall components by edge-localized modes (ELMs) under high-confinement (H-mode) operation. For devices larger than ITER, even the steady-state fluxes can become unacceptably large in ELM-quiescent plasmas. We propose driving toroidally non-axisymmetric current through the scrape-off layer (SOL) plasma both (i) to broaden the SOL and reduce the SOL pressure gradient by driving radial convection in the divertor [1,2] and (ii) to affect the ELM stability threshold by driving a resonant magnetic perturbation (RMP) field of sufficient amplitude to control the pedestal pressure gradient [3-5]. This technique can potentially achieve both goals in a synergistic fashion because the asymmetric electrostatic potentials needed to generate convection also drive an asymmetric SOL current parallel to the magnetic field. This current, in turn, generates a magnetic perturbation field that is highly resonant with the pitch of field lines near the separatrix. There has been experimental confirmation that each technique can be independently successful when using biasable electrodes to generate the potential and external coils to generate the RMP field. Convection generated by direct biasing was shown to significantly spread the SOL plasma on MAST [6] where this technique was shown to reduce the peak heat flux at the target plate. For NSTX, electrodes at the midplane were shown to locally move the SOL plasma in the radial direction [7]. First results of experiments to test the effect on the NSTX divertor are reported below. RMPs generated by external coils have been demonstrated to produce sufficient transport to reduce the edge pressure gradient below the peeling-ballooning

MHD stability threshold on DIII-D if the amplitude of the resonant spectral component exceeds a threshold of order $\delta B/B \geq 10^{-4}$ [8,9]. External coils have been used to destabilize ELMs or induce small ELM regimes on other devices at similar thresholds [10-12].

In a fusion reactor, the needed hardware is subjected to high temperatures and large forces and is severely complicated by engineering constraints in a high field and high neutron-flux environment. In many active schemes, generation of the necessary potentials is still challenging due to the possibly substantial power requirements and the possible need for internal insulators. A number of reactor-relevant passive current-drive techniques were identified in Ref. [1] that have significant advantages when compared to the use of external coils or electrodes including: varying the angle of the target plates with respect to the magnetic field, varying the conductivity or secondary electron emission coefficient of the plate material, and differential pumping or injection of neutral gas. We analyze the technical feasibility of passive methods through a combination of analytic and reduced numerical models using the UEDGE simulation code [13]. In a reactor, the neutral mean-free path will be small compared to the width of the dense plasma region across the target; thus, injecting gas through small channels or narrow slots near the target plate can generate a localized source. Neutral fueling and enhanced radiation at one of the target plates will locally reduce both the electron temperature and the floating potential. The thermal asymmetry drives a difference between the sheath potential and the floating potential and drives a parallel current between the end plates. This technique was successful at driving 20-40% of the ion saturation current in a flu-tube model of the SOL [14]. The electron temperature at the target plate is predicted to be most sensitive when the divertor plasma is at the border between attachment and detachment [15] or close to the transition to a highly radiative state [16].

2. Spatial structure of non-axisymmetric SOL perturbations

Both perturbation fields can be driven through the SOL itself, as close as to the edge as possible, because potential differences as large as the electron temperature T_e and parallel currents as large as the parallel ion saturation current $J_{sat}=en_ec_s$ can be driven if the sheath potential differs from the floating potential by $O(T_e/e)$ where e is the electron charge, n_e is the electron density, and c_s is the sound speed. If the sheath potential varies toroidally, both non-axisymmetric convection and non-axisymmetric SOL current will be generated. The perturbed current must be strongly aligned with the magnetic field lines because the effective cross-field conductivity is small compared to the parallel conductivity [2,17]. The perpendicular currents are smaller by $O(k\rho)$ where ρ is the ion gyro-radius and k is the characteristic perpendicular wavenumber of the perturbation. This implies that the parallel wavenumber for variation of the perturbation can be considered negligible $k_{\|}\sim 0$. In terms of magnetic flux coordinates $\{\psi, \theta, \zeta\}$, the parallel current must be a function of the magnetic flux ψ and the field line label $\zeta_0=\zeta-q\theta$, where ζ is the cylindrical toroidal angle, θ is the straight field line poloidal angle, and q is the safety factor. Near the X-point, the poloidal magnetic flux can be expanded as $\psi=RB_p'xy$ where x

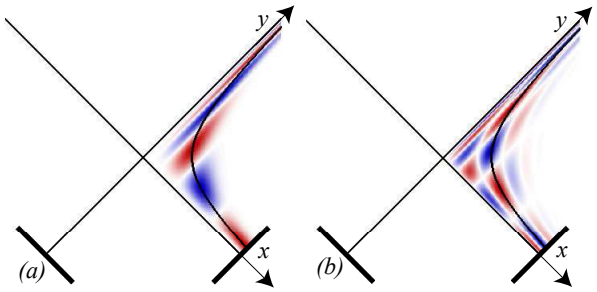

FIG. 1. Field-aligned structure of the non-axisymmetric parallel current and electrostatic potential in the X-point region generated by perturbations to the divertor plasma. On the target plate, the perturbation varies (a) in the toroidal direction only and (b) in both the radial and the toroidal directions.

and y are coordinates aligned with the branches of the separatrix, R is the major radius and RB_p' is the gradient of the poloidal magnetic field at the X-point. The field line label can be expanded as $\zeta_0=\zeta-q_*\log(y/x)$ where $q_*=B_t/RB_p'$ is the dimensionless parameter that measures the ratio of toroidal to poloidal field line motion and B_t is the toroidal magnetic field. Figure 1 shows a cross-section of the characteristic phase pattern near the X-point for two different scenarios. If the electric potential $\Phi=\Phi_0(\psi)\cos(n\zeta)$ varies with toroidal mode number n on the divertor target plate, then it must vary as $\Phi\sim\Phi_0(\psi)\cos(n\zeta_0)$ in the plasma as in Fig. 1a. In order to drive the series of convection cells shown in Fig. 1b, the radial dependence of the perturbation on the target plate must be sinusoidal as well $\Phi_0(\psi)\sim\cos(k_xk_y\psi)$. The figure clearly shows that the perpendicular wavelengths are both stretched $k_y\sim\exp(-\zeta/q_*)$ and contracted $k_x\sim\exp(+\zeta/q_*)$ by the action of magnetic shear near the X-point. The development of such fine scale structure eventually causes cross-field conduction to become an equal player in current continuity near the separatrix above the X-point and causes a reflection of parallel current from this region due to kinetic or dissipative effects. Reference [5] estimated the radial width of the "shadow" region above the X-point where the perturbation cannot travel either due to the development of perpendicular scales below the ion-gyroradius or due to the decay caused by a combination of viscous and resistive dissipation.

3. Optimization for enhanced convection

Enhanced convection in the divertor can help to mitigate the large steady-state heat fluxes that are naturally generated in a reactor by generating a large-amplitude steady-state convection pattern or by inducing secondary instabilities that induce additional turbulent transport. A typical steady-state pattern of laminar convection cells is shown in Fig. 1b. The perturbation must be super-imposed upon the equilibrium potential which, in the SOL, is primarily determined by the floating potential $\Phi_{float}=\Lambda T_e$, where the sheath coefficient is $\Lambda=\frac{1}{2}\log(V_{Te}^2/2\pi c_s^2)\sim$2-4 and $V_{Te}=(T_e/m_e)^{1/2}$ is the electron thermal speed with electron mass m_e. In order to generate a convection cell, there must be an O-point in the flow. Thus, the gradient of the perturbed potential must be large enough to cancel the gradient in the background $e\Phi/T_e>\Lambda/k_xL_{Te}$ where $L_{Te}=T_e/T_e'$ and k_x is the radial wavenumber of the perturbation. For potential perturbations of order ΛT_e, a radial wavelength that is 2π times the SOL T_e decay length would be required. If convection cells are generated in the SOL, transport will typically be dominated by steady-state convection rather than by anomalous diffusion due turbulence. The relative importance can be measured by the ratio of the diffusion time to the eddy turn-over time: the dimensionless Péclet number $P=(e\Phi/T)/(D/\rho V_T)$, where D is the diffusion coefficient, $V_T=(T/m)^{1/2}$ is the thermal speed with temperature T and mass m, and $\rho=mV_T/eB$ is the gyroradius. Even for Bohm diffusion $D\sim\rho V_T/16$, the large Péclet regime only requires $e\Phi/T>1/16$. For $P<1$, the effective diffusivity D^* is only enhanced quasilinearly, but for $P>1$, the effective diffusivity D^* is greatly enhanced $D^*\sim DP^{1/2}=(e\Phi/T)^{1/2}(D/\rho V_T)^{1/2}$ [18]. The convection cells are also effective at spreading heat if the eddy turn-over time is shorter than the parallel transit time L_c/V_T where L_c is the connection length. The maximum rotation frequency $\Omega_0=p_xk_y\Phi/B$ occurs at the center of the cell where the radial gradient is $p_x=k_x-\Lambda/L_T$. Thermal convection will dominate thermal conduction if $e\Phi/T >> 1/p_xk_y\rho L_c$. Thus, convection is optimized at wavelengths small enough to generate substantial vorticity, but large enough to entrain the coherent structures that comprise edge turbulence. Generating or suppressing a new instability can also be an effective way to control the divertor plasma. Kelvin-Helmholtz modes can directly tap free energy in the sheared flows generated by the convection cells. However, some of the most virulent divertor instabilities are anticipated to be the mode that is driven by the large electron

temperature gradient in the presence of finite sheath resistance [17,19]. Tilting the target plates with respect to the magnetic field will strongly affect the stability of this mode [17] in addition to generating a toroidal asymmetry that can drive steady-state convection [1].

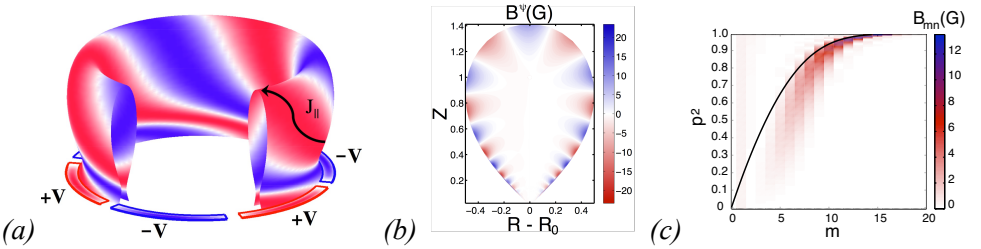

FIG 2. (a) The parallel surface current density $K_{||}$ resulting from biasing the target with 6 segments. (b) The magnetic perturbation field in the two-wire model of a plasma equilibrium produced by $K_{||}$=10 kA/m at a higher mode number. (c) At the edge (p^2=1), the poloidal spectrum is peaked near m=qn (black line).

4. Optimization for resonant magnetic perturbations

The parallel SOL current produces a magnetic perturbation δB that is largest near the plasma edge. The resonant spectral component of δB can exceed the present experimental ELM control threshold if the efficiency of driving current from divertor to SOL is optimized by choosing the appropriate width and phasing of the biasing region at the target plate [3,4]. The needed spectrum can be generated efficiently because the SOL current is as close to the plasma edge as possible and is primarily parallel to the equilibrium field, which produces a primarily perpendicular perturbation. This ensures that δB is almost entirely resonant with the pitch of the equilibrium field lines, i.e. the helicity matches the safety factor so that $n/m=q$ where n is the toroidal mode number and m is the poloidal mode number. The perturbation amplitude can be estimated to be of the same order as the discontinuity in the tangential field across the current channel. If the total surface current density integrated across the width of the SOL is $K_{||}=\int J_{||}dr$, this yields the estimate $\delta B=\mu_0 K_{||}/2$ and implies that, along the separatrix, the relative amplitude is proportional to the local flux expansion $\delta B/B \propto 1/RB_p$. This scaling arises because $J_{||} \propto B$ due to current continuity $0=\nabla\cdot\mathbf{J}\sim\mathbf{B}\cdot\nabla J_{||}/B$, while the width of the current channel increases with flux expansion so that $K_{||} \propto B/RB_p$. The parallel current pattern that is produced by biasing a thin region near the strike point in order to create an n=3 perturbation is shown in Fig. 3a. This current produces a perturbation inside the plasma, as shown in Fig. 3b (at somewhat higher mode number) and Fig. 3c displays the resulting perturbation spectrum for a simple two-wire model of the equilibrium field. Magnetic perturbations that are intended to affect the region inside the separatrix are optimized at long toroidal and radial wavelengths. As discussed in Sec. 2, this ensures that the SOL current can travel past the X-point toward the midplane. Moreover, if the poloidal wavenumber k_y is too short, as in Fig. 1b, the perturbation will only reach a distance of order $1/k_y$ across the separatrix. The optimal radial width in x for the current channel is the "coherence width" $\sigma=\psi\ \sinh(\chi/\pi nq_*)$, measured in units of flux, which vanishes as the strike point is approached [3]. Here, χ is the "phasing" of the perturbation and varies from π for a divertor with long legs to $\pi/2$ for a divertor with short legs. Even if the phase across the target is uniform radially, as in Fig. 1a, the current density near the separatrix develops finely layered oscillations in phase if the width of the current channel is greater than σ. These oscillations reduce the net surface current in the SOL relative to that in the divertor leg. Estimates for the "efficiency" ε_{SOL} of coherent current drive are given in Ref. [3]. For a wide current channel with a step-wise constant current density, the efficiency is only equal to the amount of current in a single coherent layer $\varepsilon_{SOL}\sim\chi/\pi nq_*$. Techniques that optimize the amplitude of coherent SOL current drive must balance the ion saturation current profile at the target against efficient geometric coupling.

5. Preliminary results of divertor biasing experiments on NSTX

Two pairs of 4 cm x 1.5 cm electrodes were installed in the lower outer divertor region of NSTX as shown in Fig. 3a,b in order to investigate the effect of biasing on the local plasma. Each electrode can be biased up to +100 V/40 A, or -100 V/10 A, and was modulated on/off at 50 Hz. The local plasma response was measured by a nearby array of Langmuir probes and by a fast camera viewing this region from above using visible light filters. The divertor plasma near the target plates is normally dominated by large turbulent fluctuations that appear as toroidally elongated filaments [20]. These filaments can be seen in filtered LiI light in the camera frames shown in Fig. 3c,d. When the outer electrode of the toroidal pair (Fig. 3a) was biased to +90 V, drawing an average current of ~10 A, these filaments were systematically deflected ~1 cm radially outward near the electrode, as seen in Fig. 3d. However, the deflection does not appear to extend beyond the electrodes, and no significant changes due to this biasing were seen in the Langmuir probes ~3 cm toroidally downstream. In this case, the electrodes were ~15 cm radially outside the outer strike point radius, so the biased flux tube was relatively far from the separatrix, yet the electron power flux to the electrode was ~1 MW/m^2, and the electrode surface temperature rise was visible in the cameras within ~0.1 s. The interpretation of these results is in progress.

(a) *(b)* *(c)* *(d)*

FIG 3. Two pairs of biasable electrodes were recently installed on the NSTX outer divertor plates: (a) toroidally oriented pair and (b) radially oriented pair. The white surfaces are the newly installed liquid lithium divertor plates. Top-down views of the toroidal pair in (a) as viewed in LiI light: (c) no bias and (d) ± 90 V bias. Turbulent filamentary structures are observed to bend around the outer positively biased electrode as they pass by.

6. Using neutral pumping/injection to passively generate a thermo-electric potential

The electron temperature T_e near the target plate is the key parameter that controls the thermo-electric potential. The thermo-electric potential that drives parallel current can be defined as $\Delta\Phi_{thermo}=\Delta\Phi_{float}-\int dp_e/en_e-\alpha\Delta T_e/e$ where $\alpha=0.71$ in a collisional plasma, and the difference in floating potential $\Delta\Phi_{float}=\Lambda T_e$ is the dominant term. Reference [14] calculated the ability of enhanced pumping and/or enhanced neutral gas injection to effectively manipulate both n_e and T_e in a flux-tube model of the SOL. For specified fueling conditions, the density and temperature must generally satisfy an inverse relationship. The boundary condition for total particle flux at the target plate is $\Gamma_t=(1-R_i)n_ic_s+(1-A_n)n_nV_{Tn}/(2\pi)^{1/2}$ where n_n is the neutral density, R_i is the ion recycling coefficient, A_n is the neutral albedo, and V_{Tn} is the neutral thermal speed. One can parameterize $\Gamma_t/n_ec_s=\delta$, where δ~1–10% depends on the material composition of the target plates and the geometry of any neutral injection and pump locations, but varies relatively weakly with temperature. The material properties of the target plate tiles determine R_i and can effectively control the asymmetry, as shown in Ref. [14]. However, in steady-state conditions, the walls become fully saturated, so that R_i~1 and it is only possible to manipulate the pumping and injection of neutrals. The heat flux reaching the target plate can generally be parameterized as $Q_t=\gamma n_ec_sT_e$ where the heat flux transmission factor is γ~5–10. Thus, at fixed fluxes the implicit relation $n_eT_e^{3/2}=(Q_t\delta/\gamma)(m_i/(1+T_i/T_e))^{1/2}$ holds where the right-

hand side depends weakly on temperature. In practice, it is not the particle flux Γ_t, but the midplane pressure p_m or midplane density n_m that is typically kept fixed. In this case, the divertor plasma pressure can be parameterized as a fraction f of the upstream plasma pressure [15] which yields the alternate scaling $n_e T_e = f p_m/2(1+T_i/T_e)$. The fraction f~1 varies relatively weakly with temperature above 10 eV, but transitions to small values f~0.01-0.1 in the detached state once neutral pressure becomes an important part of momentum balance (c.f. Fig. 7 of Ref. [15]). To determine the relation at fixed midplane density n_m, the variation of midplane temperature T_m due to thermal conduction and radiative losses must be included. If the divertor T_e is too high, the SOL temperature is nearly constant, little power can be radiated, and the profiles are too stiff to manipulate. If the divertor T_e is much lower than the midplane T_m and radiative effects are weak, then T_m is set by the heating power and the previous scaling holds with $p_m = n_m T_m$. Strong radiative losses can make the midplane temperature T_m and divertor temperature T_e tightly coupled [16]. The target plate plasma is most sensitive when the divertor is close to the transition to a highly radiative state or at the border between attachment and detachment. Near these bifurcation points, the plasma may be able to spontaneously transition to a naturally non-axisymmetric state [16].

7. Preliminary modeling of SOL current generated by divertor asymmetries in ITER

In the following, the generation of SOL current by an asymmetry in T_e between the inner strike point (ISP) and outer strike point (OSP) is studied using a 2D numerical model of the ITER divertor. A full assessment of non-axisymmetric current drive techniques will require a 3D calculation. However, low toroidal mode numbers were previously identified as most promising, and the 2D model quantifies the ability of passive techniques to alter the naturally generated axisymmetric poloidal asymmetry in T_e. Here, the UEDGE code [13] is used to model the plasma as a "flux-limited" Braginskii plasma with the addition of anomalous diffusion coefficients assumed to be generated by turbulence. The simulation is based on the standard ITER scenario which has a toroidal field B_t=5.3 T at major radius R=6.2 m and a plasma current I=5.4 MA. The model for the electric potential neglects cross-field conductivity so that $\mathbf{B}\cdot\nabla(J_{||}/B)=0$, where the parallel current is set by parallel electron momentum balance. The divertor region of the computational mesh (28 radial x 64 poloidal points) is shown in Fig. 4a. The density and temperatures are fixed on the innermost flux surface at ψ=0.95 (R-R_{sep}=-6 cm on the outer midplane) with $n_{i,core}=6\times10^{19}$ m^{-3} and input power P_{core}=100 MW split equally into electron and ion channels. The outer edge of the SOL is at ψ=1.035 (R-R_{sep}=4 cm on the outer midplane). The transport model has a constant radial particle diffusivity D=0.3 m^2/s, perpendicular viscous diffusivity η=1 m^2/s, and radial thermal diffusivity χ=1 m^2/s. Carbon impurities are assumed to be present at a fixed fraction of 3%. Neutral pumping and/or injection zones are defined on either side of the private flux region (shown in Fig. 4a). For the reference case, both pumps have 2% efficiency, A_n=98%. The strong tilt angle of the ITER target plates forces neutrals to accumulate in the collisional private flux region (PFR). The high ion temperature and low neutral density (Fig.

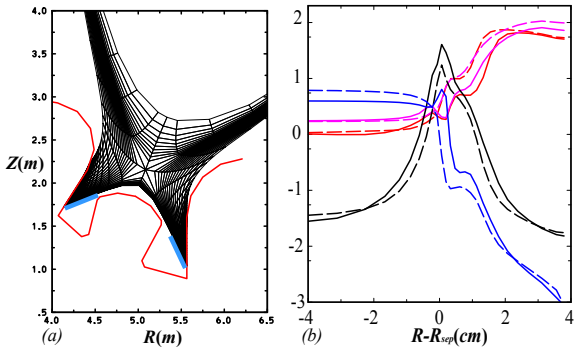

FIG. 4. (a) The ITER mesh (black), approximate geometry of the divertor baffle (red), and pump/injector regions (blue). (b) The plasma conditions on the target plate in the reference case vs. distance on the outer midplane: log_{10} scale for T_e (eV, red), T_i (eV, magenta), n_i (10^{20}m^{-3}, black), and n_n (10^{20}m^{-3}, blue).

4b) on the outer side of the plate increases the mean-free path to 5-10 cm, which makes it difficult to control the neutral density in this region. The poloidal asymmetry in T_e drives a toroidally symmetric current from the hotter OSP to the colder ISP, $I_{||}$=285 kA at the ISP, 5.42% of I_{sat}. The current density $J_{||}$ (red curves in Fig. 5) actually has 2 peaks. This implies that a surface current $K_{||}$=11 kA/m^2 is driven by the thermo-electric potential Φ_{thermo}=-47.4 V (averaged over the $J_{||}$ profile). This surface current can potentially produce δB~67 G or $\delta B/B$~8.7x10^{-4}. If the OSP plate is biased to +50 V, a parallel current of $I_{||}$=742 kA is collected at the inner plate, 15.5% of I_{sat}. In this case, the radiated power fraction drops to 32.4% and there is 7.7 MW of Ohmic heating, of which 2.3 MW must be supplied by the biasing system. If the ISP target plate is biased to +50V, $I_{||}$=-149kA of current is driven toward the OSP, 4.2% of I_{sat}, which represents an equal change in current amplitude. However, the Ohmic heating power is only 1.3 MW and only 0.72 MW needs to be supplied by the biasing system.

Thus, modest biasing can drive $K_{||}$~15 kA/m at the target which would generate $\delta B/B$~2x10^{-3}. The most efficient place to affect the neutral density is in the PFR where the neutral density is high. If the ISP pumping efficiency is increased to A_n=0.9, the current is reduced to $I_{||}$=207 kA, 5.4% of I_{sat}. If the OSP pumping efficiency is increased to A_n=0.9, the current is increased to $I_{||}$=365 kA, 7.2% of I_{sat}. If the OSP pump is blocked (A_n=1), then $I_{||}$=191 kA is driven, 3.1% of I_{sat}, but if the ISP pump is blocked, there is little change in $I_{||}$=284 kA, now only 3.1% of I_{sat}. Thus, differential pumping can possibly drive $K_{||}$~3-4 kA/m which would generate $\delta B/B$~2x10^{-4}. Neutral injection can be used to enhance this effect and can generate roughly ~10-20% of this δB at neutral injection currents of 0.1-1 kA. Thus, neutral pumping and injection can marginally exceed the anticipated ELM control threshold.

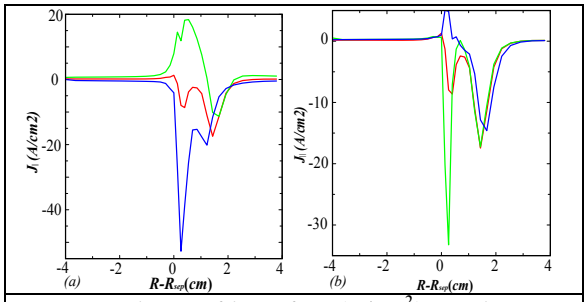

FIG. 5. The profiles of $J_{||}$ (A/cm^2) on the OSP for: (a) reference case (red), ISP biased to +50 V (green), OSP biased to +50 V (blue); (b) reference case (A_n=98%, red), enhanced OSP pumping (A_n=90%, green), no OSP pumping (A_n=100%, blue).

8. Conclusion

In conclusion, the possibility of using non-axisymmetric perturbations to control the edge plasma and SOL profiles and stability is under active theoretical and experimental investigation. Electrostatic perturbations can be used to form a standing convection pattern or to induce instabilities that spread the steady-state heat and particles fluxes near the strike points. Convection requires a potential difference that exceeds the background and is optimized at toroidal and radial mode numbers that are large enough to ensure that the convective flux exceeds the background level of turbulent fluxes. Magnetostatic perturbations may also be generated in order to control particle and heat fluxes and can, in principle, exceed the threshold for ELM control. Magnetic perturbations are optimized at low toroidal and radial mode numbers in order to generate a coherent current perturbation that travels well beyond the X-point and into the SOL. The possibility of using passive current drive techniques that rely on neutral pumping and injection was studied for a model of the ITER divertor. Due to ITER's sharply-inclined target plates, the asymmetry between inner and outer strike points is relatively stiff and the achievable difference in SOL current is only ~2-5% of the total ion saturation current. While the techniques studied here can potentially exceed the ELM control threshold, alternate divertor configurations and more efficient current-drive methods should be pursued as a topic of further exploration.

Acknowledgements

This work was performed for the US Department of Energy under the auspices of the Lawrence Livermore National Laboratory under contract DE-AC52-07NA27344.

References

[1] COHEN, R.H., RYUTOV, D.D., "Plasma convection induced by toroidal asymmetries of the divertor plates and gas puffing," Nucl. Fusion **37** (1997) 621.
[2] RYUTOV, D.D., et al., "On the possibility of inducing strong plasma convection in the divertor of MAST," Plasma Phys. Control. Fusion **43** (2001) 1399.
[3] JOSEPH, I., COHEN, R.H., RYUTOV, D.D., "Driving toroidally asymmetric current through the tokamak scrape-off layer. I. Potential for edge localized mode suppression," Phys. Plasmas **16** (2009) 052510.
[4] JOSEPH, I., "Driving toroidally asymmetric current through the tokamak scrape-off layer. II. Magnetic field structure and spectrum," Phys. Plasmas **16** (2009) 052511.
[5] JOSEPH, I., "Magnetic perturbation spectrum produced by non-axisymmetric scrape-off layer current and the X-point shadow," Contrib. Plasma Phys. **50** (2010) 331.
[6] COUNSELL, G.F., et al., "Exhaust, ELM, and halo physics using the MAST tokamak," Nucl. Fusion **43** (2003) 1197.
[7] ZWEBEN, S.J., et al., "Local scrape-off layer control using biased electrodes in NSTX," Plasma Phys. Control. Fusion **51** (2009) 015012.
[8] BURRELL, K.H., et al., "ELM suppression in low edge collisionality H-mode discharges using n = 3 magnetic perturbations," Plasma Phys. Control. Fusion **47** (2005) B37.
[9] EVANS T.E., et al., "Edge stability and transport control with resonant magnetic perturbations in collisionless tokamak plasmas," Nature Phys. **2** (2006) 419.
[10] LIANG, Y., et al., "Active control of type-I edge-localized modes with n = 1 perturbation fields in the JET tokamak," Phys. Rev. Lett. **98** (2007) 265004.
[11] CANIK, J.M., et al., "ELM destabilization by externally applied non-axisymmetric magnetic perturbations in NSTX," Nucl. Fusion **50** (2010) 034012.
[12] NARDON, E., et al., "Edge localized mode control experiments on MAST using resonant magnetic perturbations from in-vessel coils," Plasma Phys. Control. Fusion **51** (2009) 124010.
[13] ROGNLIEN, T.D., et al., "A fully implicit, time dependent 2-D fluid code for modeling tokamak edge plasmas," J. Nucl. Mater. **196-198** (1992) 347.
[14] JOSEPH, I., ROGNLIEN, T.D., "Assessment of thermo-electric techniques for scrape-off layer current drive in flux-tube geometry," J. Nucl. Mater. (in press).
[15] PITCHER, C.S., STANGEBY, P.C., "Experimental divertor physics," Plasma Phys. Control. Fusion **39** (1997) 779.
[16] STAEBLER, G.M., "The critical point for the onset of divertor energy flux asymmetry in tokamaks," Nucl. Fusion **36** (1996) 1437.
[17] RYUTOV, D.D., COHEN, R.H., "Geometrical Effects in Plasma Stability and Dynamics of Coherent Structures in the Divertor," Contrib. Plasma Phys. **48** (2008) 48.
[18] ROSENBLUTH, M.N., et al., "Effective diffusion in laminar convective flows," Phys. Fluids **30** (1987) 2636.
[19] BERK, H.L., et al., "Electron temperature gradient induced instability in tokamak scrape-off layers," Nucl. Fusion **33** (1993) 263.
[20] MAQUEDA, R.J., et al., "Intermittent divertor filaments in the National Spherical Torus Experiment and their relation to midplane blobs," Nucl. Fusion **50** (2010) 075002.